Available online at **www.joac.info**

ISSN: 2278-1862

Journal of Applicable Chemistry

2019, 8 (4): 1657-1664

(International Peer Reviewed Journal)

Electrochemical Synthesis and Factors Affecting the Photocatalytic Behaviour of ZnO-V_2O_5 Nanostructures

Jenice Jean Goveas[1], Sandhya Shetty[2], Naveen Praveen Mascarenhas[1], Renita Mishal D'Souza[1]and Richard Adolf Gonsalves[1]*

1. Department of Chemistry, St. Aloysius College (Autonomous), Mangalore-575003, **INDIA**
2. St Agnes Centre for Post Graduate Studies and Research, Mangalore-575002, **INDIA**

Email: richieag@yahoo.com

Accepted on 9th June, 2019

ABSTRACT

An attempt is made to establish the role of electrochemically generated nanostructures of Zinc-Vanadium oxides as photocatalysts by investigating 2 commonly used dyes Methylene Blue (MB) and Eriochrome Black-T (EBT) under UV light. Mixed metal oxides of Zinc and Vanadium (ZnO and V_2O_5) nanostructures (ZVO) were synthesized using a facile electrochemical-thermal method by electrolyzing an aqueous solution of sodium bicarbonate and sodium vanadate using sacrificial Zinc electrodes in an undivided pyrex cell under potentiostatic conditions at room temperature. The resulting particles were calcined at different temperatures. The role of 3 different surfactants-Cetyltrimethyl ammonium bromide (Cetrimide), Sodium dodecyl sulphate (SDS) and Polyethylene glycol (PEG) during synthesis was also investigated to enhance their photocatalytic action. Characterization of these nanoparticles was carried out using powder XRD, SEM, TEM, FTIR, TGA and UV-Visible spectra. Photocatalytic behavior of the prepared and pulverized samples was investigated using different dyes like MB and EBT. The effect of operating parameters like temperature and initial dye concentration on the rate of dye degradation was studied. High degree of decolorization was achieved under optimum experimental conditions suggesting photochemical degradation of dyes by nanostructures of ZnO-V_2O_5. The photodegradation results indicate high degree of decolorization and resultant mineralization of the organic dyes. It indicates that this technique could be envisaged for treatment of effluents mainly from textile industries.

Graphical Abstract

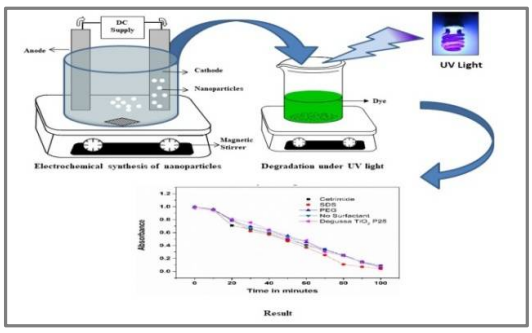

Keywords: Electrochemical, Zinc, Vanadium, Nanostructures, Photocatalyst, Surfactant.

INTRODUCTION

Although electrode position has been one of the oldest techniques for deposition prevailing from the time of Alexander Volta (1800) this technique has not received the attention it requires [**1, 2**]. Semiconductor oxide materials such as ZnO, CuO, TiO_2, V_2O_5, SnO_2, ZrO_2 and WO_3 are attractive photocatalysts because they are not only environmentally sustainable but also show high catalytic efficiency in degradation of various environmental pollutants such as pesticides, detergents, dyes and volatile organic compounds[**3, 4**]. A number of methods including physical, chemical and biological techniques have been developed for the degradation of organic compounds [**5, 6**]. Among the new oxidation methods or advanced oxidation processes (AOP), heterogeneous photocatalysis stands out as an emerging destructive technology resulting in the complete mineralization of most of the organic pollutants [**7**]. Among the oxide-based semiconductors ZnO has good electron portability, luminescence coupled with large exciton binding energy (60 MeV) [**8**]. V_2O_5 is an efficient semiconductor with narrow band gap energy (~2.2 eV) used as an active catalyst for the photodegradation of organic pollutants [**9**]. It has commercial applications in lithium-ion batteries, gas sensors and optoelectronic devices [**10**]. Nevertheless, rapid recombination of photogenerated electron–hole pairs during the photocatalytic process reduces the operative degradation capacity. Several efforts have been made to overcome this problem which includes coupling of two semiconductors. Using coupled semiconductor photocatalysts augments the electron–hole separation via interfacial charge transfer between the two semiconductors and substantially improves photocatalytic degradation of the dye [**11**].

This paper discusses a simple, lowcost hybrid electrochemical thermal method to generate a large quantity of zinc oxide-vanadium pentoxide nanoparticles (ZVO). Heterometal oxide nanoparticles, which are solid solutions containing a certain amount of cation vacancy, with a uniform particle size less than 50 nm and huge surface area were synthesized by electrochemical deposition and calcination. The prepared and pulverized structures were characterized with different analytical and spectroscopic techniques which include-Powder X-Ray Diffraction (XRD), scanning electron microscopy (SEM), Fourier transform infrared spectroscopy (FT-IR), Transmission electron microscopy (TEM), UV-Visible spectroscopy and thermogravimetric analysis (TGA). An attempt has been made to establish the role of the synthesized ZVO nanoparticles as potential photocatalysts for the destruction of dyes present in aqueous textile effluents using 2 model pollutants MB and EBT by degradation under UV light. The factors affecting their photocatalytic activity is also discussed.

MATERIALS AND METHODS

High purity zinc metal plates (99.99%), Sodium bicarbonate (AR grade: 99.5%), Sodium vanadate (AR grade: 98.5%) were purchased from Sisco Research laboratories, Mumbai and MB and EBT from S.D. Fine Chemicals Ltd, India were used as received. Millipore water (specific resistance, 15 mΩ cm at 25°C, Millipore Elix 3 water purification system, France) was used for the preparation of the electrolyte solution. During electrolysis, constant voltage of 12V was supplied using a DC power supply (Model PS 618 potentiostat/galvanostat 302/2 A). For filtration Whatman filter paper No. 41 was used.

Synthesis of Nanocomposites: ZVO nanoparticles were synthesized using a standard electrochemical technique [**12**]. Prior to electrolysis, the Zn plates were activated using dilute HCl followed by washing with millipore water. The electrolyte was a 400ml solution taken in a pyrex vessel containing $NaHCO_3$ to increase the conductance and Sodium Vanadate for deposition. It was introduced into a rectangular undivided cell where pure Zn plates were used as both cathode and sacrificial anode. The electrolysis was carried out for about one hour under potentiostatic conditions; a constant voltage of 12V was supplied by a DC power supply (model PS 618 potentiostat/galvanostat 302/2 A) with constant stirring at 500 rpm.

The pH of the electrolyte was recorded before and after the electrolysis. Optimum pH of 10 was maintained using a buffer. The white precipitate formed was filtered (by Whattman filter paper No.41) to be isolated from the solution. The electrolysis was also carried out in the presence of 3 different surfactants-cetrimide, PEG and SDS just above their critical micellar concentration. The obtained powder was calcined at different temperatures for an hour.

Assessment of Photocatalytic Activity: Photocatalytic tests were performed at an ambient temperature on the samples for decomposition of MB and EBT solution. A pyrex beaker (250 mL) was used as the photo-reactor vessel. An amount of 0.05 g of ZnO samples was added into 100ml of 1×10^{-5} M aqueous MB solution. The solutions were magnetically stirred in the dark for 10 min, and then they were irradiated A high pressure mercury vapour lamp (HPML) of 125 W (Philips, India) was placed inside the jacketed quartz tube. To avoid fluctuations of the input light intensity, a supply ballast and capacitor were connected in series with the lamp. Water was circulated through the annulus of the quartz tube to avoid overheating of the solution. Synthesized ZVO nanoparticles of varying sizes were added to 100 mL dye solution (10 ppm), with continuous stirring at 500 rpm for homogeneity. 100 mL of the solution (ZVO and MB) was taken in the beaker under continuous stir to ensure the uniform suspension of the catalyst. The lamp radiated predominantly at 365 nm, corresponding to photon energy of 3.4 eV and photon flux of 5.8×10^{-6} mol of photons s^{-1}. Prior to illumination, the suspension of ZVO was magnetically stirred for 2 h in dark to establish absorption/desorption equilibrium. Aliquots were collected from the reaction beaker at regular time intervals, centrifuged to remove particles and the concentration of dye in solution and degradation ratio was plotted as a function of time by monitoring the changes of absorbance using a UV-Visible double beam spectrophotometer. Maximum absorption for MB and EBT was at 660 nm and 568 nm respectively. The degradation of the synthesized photocatalyst was compared with the standard Degussa TiO_2-P25. Degradation was carried out varying parameters like concentration, temperature of calcination and surfactant used in the electrolytic bath.

XRD analysis of ZVO heterometal oxide Nanostructures: X-Ray diffraction data was recorded on Rigaku Miniflex 600 X-ray diffractometer with graphite monochromatized Cu-Ka (1.5406 Å) radiation. Patterns were recorded in the 2θ range from 10°to 90°at a scanning rate of 1° min^{-1}. Figure 1 shows the XRD pattern of ZVO nanoparticles. The diffraction peaks of the product can be indexed to hexagonal wurtzite structure. The crystallite size is calculated from the most intense peaks (2θ= 35°) using Scherrer formula and it was found to be 30nm. Lattice strain is 0.0088. ZnO nanoparticles also show wurtzite structure with most intense peak (2θ = 36.1°) indexed to JCPDS card no: 01-1136. The shift of the most intense peak to a lower 2θ value indicates the formation of mixed metal oxides. The diffraction peaks at 2θ values 34.3°, 36.2° indicate the formation of nanocrystalline structures compared to JCPDS card no: 75-0457.

XRD patterns of synthesized ZVO mixed metal oxide nanocomposites synthesized using SDS as an additive is represented in figure 1. Results indicate physical homogenization also confirmed through SEM.

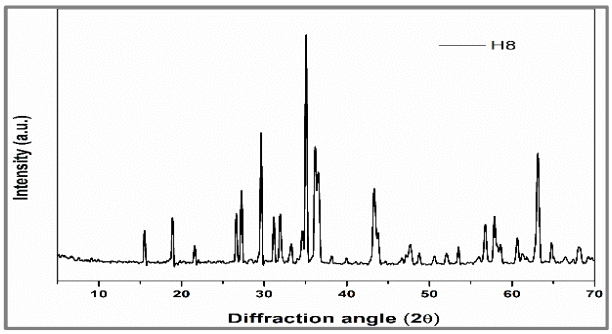

Figure 1. XRD pattern of ZVO nanoparticles synthesized using SDS as additive.

Surface morphology studies: Surface morphology was observed by using (EVO 18, Carl Zeiss, Germany) scanning electron microscopy (SEM) and shown in figure 2. It clearly shows that the particles are agglomerated to form spongy cave like structures with well-defined pores and soft agglomeration. Crystallites are interlinked and form a large network with irregular pore sizes.

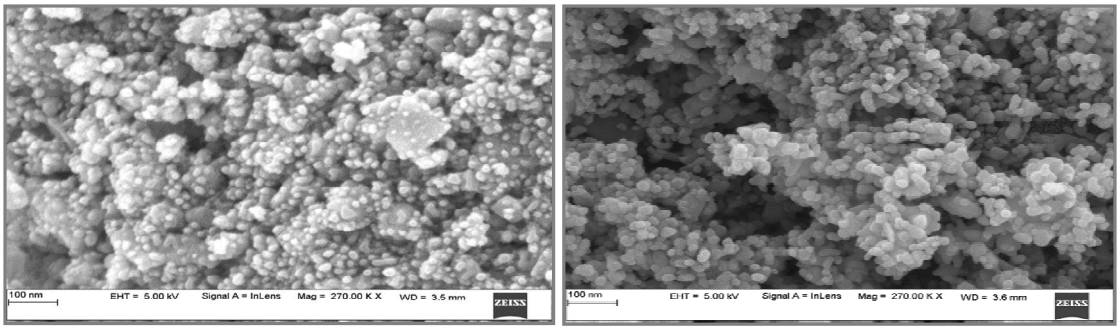

Figure 2. SEM images of ZVO nanoparticles a) in the absence of surfactants b) in the presence of SDS as additive.

Transmission electron microscope (TEM) images of selected samples were recorded (Model: JEOL 2000 FX-II) with an acceleration voltage of 200 kV. 2µL of ZnO–ethanol solution was dropped on a Cu grid with a carbon-reinforced plastic film. TEM images confirm the well embedded crystallite nature of particles and the interactive mixing of ZnO and V_2O_5 particles vital for photocatalysis. This is favorable for high degree of photocatalytic property. The average size of a primary particle is found to be 30 nm.

FTIR Spectra: The Fourier transform infrared spectra (FTIR) of the samples were recorded using Brucker-Alpha-P spectrometer. An FTIR spectrum of mixed metal oxide is shown in figure 4. A peak at 638 cm^{-1} is associated with the characteristic mode of Zn-O bond. IR absorption of V-O stretching band is observed at 829 cm^{-1} which indicates the presence of V_2O_5. The absence of VO_2 can be confirmed by the absence of peaks at 508 cm^{-1} and 714 cm^{-1}. The band at 435 cm^{-1}corresponds to Zn-O bonding and confirms the presence of ZnO nanoparticles. The band at 2351 cm^{-1} is probably due to absorption of atmospheric CO_2 and may be neglected.

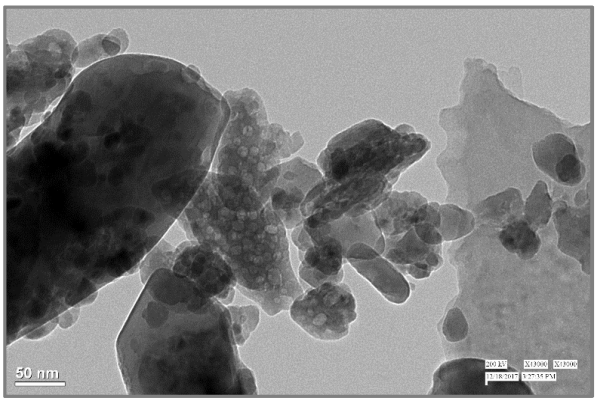

Figure 3. TEM image of ZVO calcined at 650^{0}C synthesized using SDS as additive.

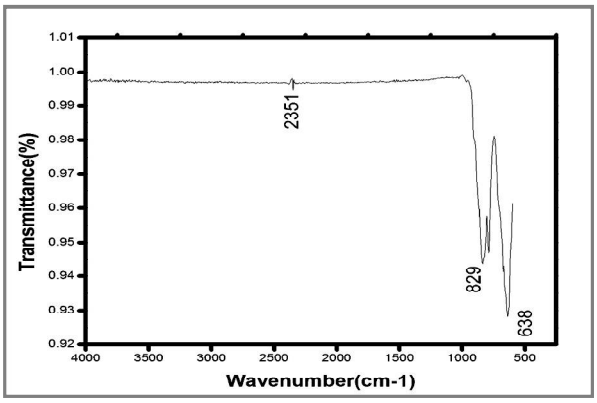

Figure 4. FTIR Spectra of ZVO calcined at 650^{0}C with SDS as additive.

RESULTS AND DISCUSSION

Band gap: Band gap study using Tauc plot is depicted in figure 5. Band gap energy for the nanocomposite is clearly shifted to a middle value closer to ZnO giving a value of 2.85eV. This may be attributed to the formation of various defect energy levels within the forbidden band.

Thermal stability assessment: Thermogravimetric analysis discloses the stability of ZVO to temperature. Weight loss of 2.998 % is detected at 900°C which could be due to voids in the sample. Weight loss indicates that the nanopowder is pure and porous (Figure 6).

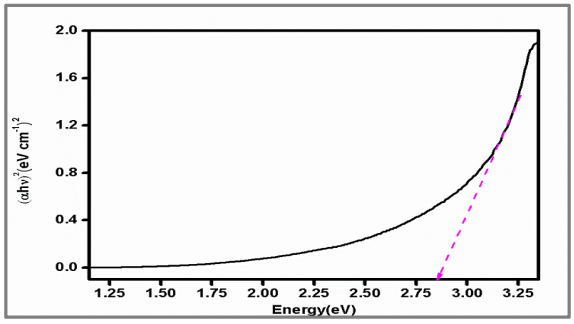

Figure 5. Tauc Plot of ZVO synthesized using SDS at650^{0}C.

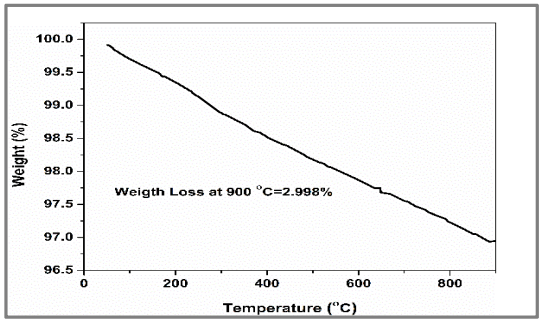

Figure 6. TGA of ZVO nanoparticles synthesized using SDS at 650^{0}C.

Evaluation of photocatalytic activity: Photocatalytic degradation of the dyes was carried out using Shimadzu UV 1800 UV-Visible spectrophotometer. Degradation graphs of MB and EBT is revealed in figure 7(a) and (b) respectively. Decolorization efficacy of 95.97% and 94.2% for MB and EBT respectively is observed for ZVO nanocomposites synthesized using SDS as additive.

$$\% \text{ of dye degradation} = \frac{A_i - A_f}{A_i} \; x \; 100$$

Where A_i and A_f are the initial and final absorptions for dye concentrations respectively.

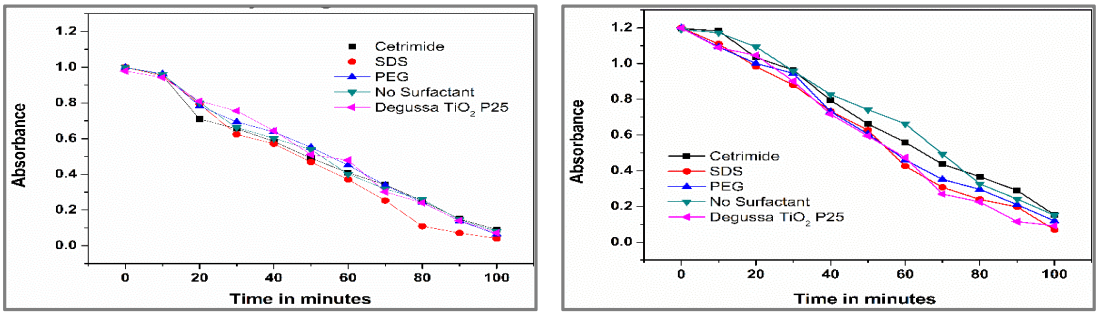

Figure 7. Photocatalytic degradation of (a) MB and (b) EBT using ZVO.

Effect of Calcination Temperature: ZVO nanocomposites synthesized at different temperatures are studied for their photocatalytic capacity to degrade the dyes. Degradation of MB and EBT nanoparticles synthesized at 40, 200, 400, 650 and 800°C are represented in figure 8 (a) and (b)

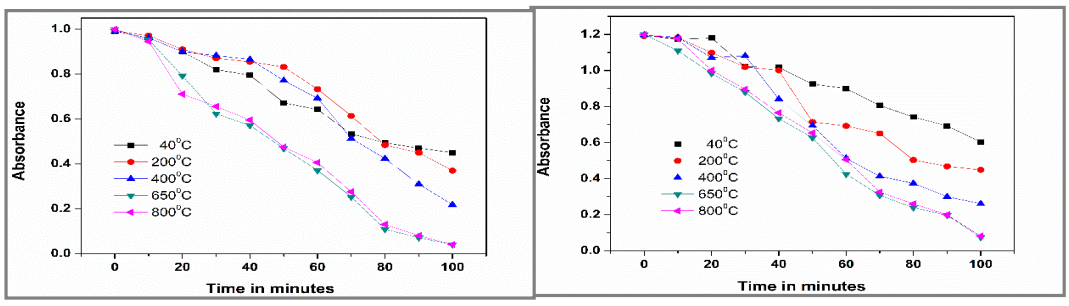

Figure 8. Photocatalytic degradation of (a) MB and (b) EBT by ZVO nanoparticles synthesized using SDS at different temperatures.

respectively. It is evident that the photocatalytic property of nanoparticles increases with increasing temperature. After 650°C, temperature did not greatly affect photocatalysis.

Effect of dye concentration: Degradation for MB and EBT using ZVO synthesized with SDS at 650°C for 3 concentrations of the dye 5ppm, 10 ppm and 25ppm is shown in figure 9 (a) and (b) respectively. Most effective degradation is seen for 10 ppm solution giving 95.9% and 92.2% degradation for MB and EBT respectively after 100 min of degradation.

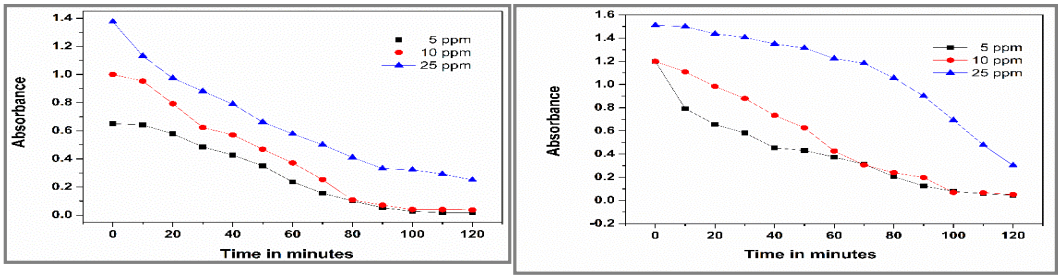

Fig. 9. Photodegradation using ZVO for varying concentrations of a) MB and b) EBT.

Kinetics of dye degradation: Kinetic studies of photocatalytic action of the synthesized ZVO is estimated from the degradation of MB and EBT, governed by the formula $-\ln C/C_0 = kt$.C is the concentration of dye at time t mins, C_0 is the initial concentration and k is the rate constant in min^{-1} [13].

Table 1. Kinetics parameters for degradation of MB and EBT

Photocatalyst	MB		EBT	
	% degradation	k x 10^{-2} min^{-1}	% degradation	k x 10^{-2} min^{-1}
ZVO + No additive	91.0282	1.5648	87.2418	1.1583
ZVO + SDS	95.9796	1.8672	92.2064	1.5874
ZVO + PEG	93.5842	1.4718	90.0425	1.4575
ZVO + Cetrimide	91.9851	1.4900	87.3489	1.0867
Degussa P25 TiO_2	92.6857	1.3946	92.3616	1.6229

The resultant rate constants are tabulated in table 1. For comparison commercially available Degussa P25 TiO_2 is used as standard. Rate constant of 0.018672 min^{-1} and 0.015874 min^{-1} is the highest for ZVO synthesized using SDS which explains the high photocatalytic activity of these nanoparticles. Higher photocatalytic activity is perhaps due to the charge separation in ZVO nanocomposite. The lesser possibility of electron-hole combination results in better photocatalytic behavior [14]. Kinetic studies of MB and EBT synthesized in the presence and absence of surfactants namely Cetrimide, SDS and PEG and is represented in figure 10 (a) and (b) respectively. Degradation follows pseudo first order kinetics.

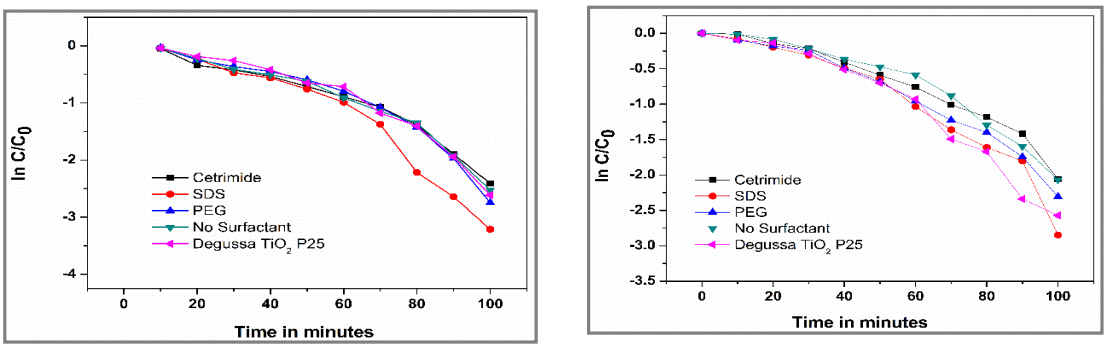

Figure 10. Kinetic studies of the degradation of (a)MB (b) EBT with different photocatalysts.

Rate constant k (min^{-1}) for the photocatalytic degradation of methylene blue and EBT process using ZVO nanocomposites is represented in figure11(a) and (b) respectively.

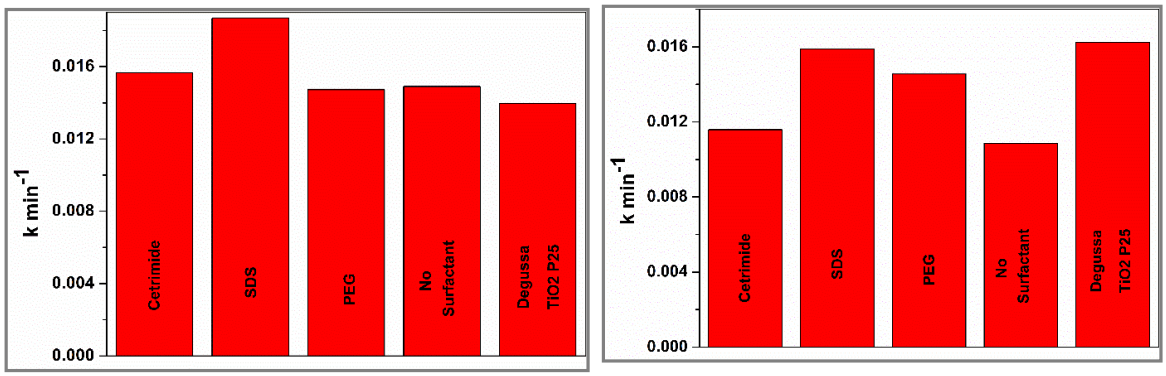

Figure 11. Rate constants for photodegradation of (a)MB and (b) EBT.

Mechanism of mixed semiconductor photocatalyst: Better photocatalytic activity of ZVO nanocomposite can be credited to electron–hole pairs generated by means of band gap excitation. When ZVO is irradiated Vanadium acts as a sensitizer to absorb the UV light. Electrons in the valence band get excited to the conduction band generating holes in the valence band. The excited electrons in the conduction band get injected to the conduction band of Zinc. This trapping of electrons thus prevents the back reaction between the photogenerated charge carriers. Valence band potential for V_2O_5 and ZnO is very close, hence photogenerated holes stay on the surface and due to electron–hole trapping enabled in the mixed semiconductor system, charge separation increases. The photogenerated electrons and holes further form the highly reactive hydroxyl radicals (OH•) [15] which oxidizes the organic dye molecules adsorbed on the photocatalyst surface.

APPLICATION

Scientific research using the electrochemical method establishes it as a convenient technique for the bulk synthesis of ZVO nanocomposites. These semiconductor metal oxides can be suitably used for the degradation of organic pollutants by nano particle photocatalytic technology in wastewater treatment.

CONCLUSION

An effective photocatalyst ZVO was successfully synthesized using a low cost and facile electrochemical-thermal process. The best photocatalyst was obtained using SDS as additive and calcined at 650°C and pH 10. It could bring about the successful photodegradation of methylene blue and Eriochrome Black-T. Kinetic studies reveal that it follows pseudo first order reaction according to Langmuir Hinshelwood mechanism**.** Hence this study is successful to demonstrate convenient use of the electrochemical-thermal path for synthesis of heterometal oxide nanocomposites which to be employed as solutions for treatment of textile industry aqueous effluents

ACKNOWLEDGEMENTS

The authors are thankful to St. Aloysius College, Mangalore for providing laboratory facility to undertake this research.

Conflict of interest: There are no conflicts to declare.

REFERENCES

[1]. W. Cun, X. M. Wang, J. C. Zhao, B. X. Mai, G. Y. Sheng, P. A. Peng, J. M. Fu, Synthesis, characterization and photocatalytic property of nano-sized Zn_2SnO_4, *J. Mater. Sci*., **2002**, 37, 2989–2996.

[2]. A.V. Prasada Rao, Evaluation of Visible Light Photocatalytic Activities of MoO_3, Cu_2O And V_2O_5 For Degradation of Rhodamine-B, Methylene Blue and Methyl Orange, *J. Applicable Chem*., **2015**, 4, 1751-1756.

[3]. K. G. Chandrappa, T. V. Venkatesha, Electrochemical synthesis and photocatalytic property of zinc oxide nanoparticles, *Nano-Micro Letters*., **2012**, 4,14-24.

[4]. Hazim Y. Al-gubury, Photocatalytic degradation of n- Hexacosane Using coupledZnO-Sb_2O_3 and tungsten lamp, *J. Applicable Chem*., **2013**, 2, 22-32.

[5]. V. K. Gupta, I. Ali, T. A. Saleh, A. Nayak, S. Agarwal, Chemical treatment technologies for waste-water recyclingan overview, *RSC Adv*., **2012**, 2, 6380–6388.

[6]. A. Fujishima, T. N. Rao, D. A. Tray, Journal of Photochemistry and Photobiology C: Photochemistry Reviews, *J. Photochem. Photobiol. C*., **2000**, 1, 1–21.

[7]. J. M. Herrmann, Water treatment by heterogeneous photocatalysis, Environmental Catalysis, F. Jansen and R. A. van Santen, Catalytic Science Series, Imperial College Press, London, UK, **1999**, 1, 171-194.

[8]. Y. J. Jang, C. Simer, T. Ohm, Comparison of zinc oxide nanoparticles and its nano-crystalline particles on the photocatalytic degradation of methylene blue, *Materials Research Bulletin*., **2006**, 4, 67-77.

[9]. B. Li, Y. Xu, G. Rong, M. Jing, Y. Xie, Vanadium pentoxide nanobelts and nanorolls: from controllable synthesis to investigation of their electrochemical properties and photocatalytic activities, *Nanotechnology*, **2006**, 17, 2560–2566.

[10]. A. Dhayal Raj, T. Pazhanivel, P. Suresh Kumar, D. Mangalaraj, D. Nataraj, N. Ponpandian, Self assembled V_2O_5 nanorods for gas sensors, *Curr. Appl. Phys*., **2010**, 10,531–537.

[11]. J. Su, X.-X. Zou, G. -D. Li, X. Wei, C. Yan, Y.-N. Wang, J. Zhao, L.-J. Zhou, J. S. Chen, Macroporous V_2O_5–$BiVO_4$ Composites: Effect of Heterojunction on the Behavior of Photogenerated Charges, *J. Phys. Chem. C*., **2011**, 115, 8064–8071.

[12]. Y. Changlin, Y. Kai, S. Qing, Y. C. Jimmy, C. Fangfang, L. Xin, Preparation of WO3/ZnO Composite Photocatalyst and Its Photocatalytic Performance, *Chi J. Cat*., **2011**, 32, 555–565.

[13]. R. Yin, Q. Luo, D. Wang, H. Sun, Y. Li, X. Li and J. An, SnO_2/gC_3N_4 photocatalyst with enhanced visible-light photocatalytic activity, *J. Mater. Sci.*, **2014**, 49, 6067–6073.

[14]. S. Adhikari, D. Sarkar, G. Madras, Highly efficient WO_3–ZnO Mixed Oxides for Photocatalysis, *RSC Adv*., **2015**, 5, 11895–11904

[15]. Yu C L, Fan C F, Yu J M, Zhou W Q, Yang K., A NiMoS Lower-Like Structure With Self-Assembled Nanosheets As High-Performance Hydrodesulfurization Catalysts, *Mater Res Bull*, **2011**, 46, 140-153.